Title: Contrail coverage over the North Pacific from AVHRR data

Corresponding author: Patrick Minnis p.minnis@nasa.gov

Institution: Atmospheric Sciences, NASA Langley Research Center

Mailing address MS 420
NASA Langley Research Center
Hampton, VA 23681-2199 USA

Second author: Rabindra Palikonda r.palikonda@larc.nasa.gov
Third author: Bryan J. Walter b.j.walter@larc.nas.gov
Fourth author: J. Kirk Ayers j.k.ayers@larc.nasa.gov
Fifth author: Hermann Mannstein hermann.mannstein@dlr.de

Institution: AS&M, Inc., Hampton, VA 23666 USA

Contrail coverage over the North Pacific from AVHRR data

Patrick Minnis[1]
Atmospheric Sciences, NASA Langley Research Center, Hampton, Virginia, USA

Rabindra Palikonda, Bryan J. Walter, J. Kirk Ayers
AS&M, Inc., Hampton, Virginia, USA

Hermann Mannstein
DLR Institut für Physik der Atmosphäre, Oberpfaffenhofen, Wessling, Germany

Abstract

An increase of air traffic over the North Pacific during the last 30 years has been accompanied by an increase in cirrus coverage. To help alleviate the uncertainty in the contribution of air traffic to the cirrus increase, an analysis of linear contrail coverage over the region has been initiated using afternoon *NOAA-16* AVHRR data taken during 4 months in 2002 and 2003. Manual evaluation of the automated contrail detection method revealed that it misclassified, on average, 23% of the contrail pixels as contrails and missed 12% of the contrail pixels. After correction for detection errors, the contrail coverage over the domain between 25° and 55°N and between 120° and 150°W varied from a minimum of 0.42% in November to a maximum of 0.56% in May, respectively. The annual mean coverage, after correcting for the diurnal cycle of air traffic, is 0.34%, a value very close to earlier theoretical estimates for the region. Contrail optical depths for the 4 months average 0.24 resulting in a mean unit contrail longwave radiative forcing of 14.2 Wm^{-2}. The contrail optical depths are twice the mean value expected from theoretical estimates.

Zusammenfassung

Eine Zunahme des Flugverkehrs ist über dem Nördlich Pazifik durch eine Zunahme in Zirrus Abdeckung während der letzten 30 Jahre begleitet worden. Zu helfen, um die Ungewißheit im Beitrag des Flugverkehrs zur Zirrus Zunahme zu erleichtern, ist eine Analyse die Abdeckung von linearem Kondensstreifen über dem Gebiet Nachmittag NOAA-16 AVHRR daten genommen in 2002 und

2003 während 4 Monate eingeleitet worden benutzend. Manuelle Abschätzung Entdeckung des automatisierten Kondensstreifens, den Methode offenbart hat, daß es fälschlich klassifiziert, im Durchschnitt, 23% vom Kondensstreifen Bildpunkten, als Kondensstreifen und 12% vom Kondensstreifen Bildpunkten verpaßt hat. Nach Korrektur für Entdeckung Fehler, die Kondensstreifen Abdeckung über der Domäne zwischen 25° und 55°N und zwischen 120° und 150°W hat sich von mindestens 0.42% zu höchstens 0.56% im Mai, jeweilig im November geändert. Die jährliche Mittelabdeckung, nachdem Korrigieren für den täglichen Zyklus des Flugverkehrs, ist 0.34%, ein Wert der sehr ist nah zu früher theoretischen Schätzungen für das Gebiet. Kondensstreifen optische Tiefen berechnen für die 4 Monate den Durchschnitt von 0.24 resultierend in einem Mitteleinheit Kondensstreifen langwellen strahlungen Zwingen von 14.2 Wm^{-2}. Der Kondensstreifen optische Tiefen sind zweimal der Mittelwert, der von theoretischen Schätzungen erwartet wird..

1 Introduction

Cirrus cloud cover has been increasing over the North Pacific since the 1970's. Although part of the increase may be due to a rise in relative humidity, some of the change is likely caused by contrails forming and spreading as a result of transoceanic air traffic. Analysis of high-resolution satellite data is required to determine the contribution by linear contrails to that increase. The air traffic passes through a region where mean cirrus cloud coverage is generally about half that observed over land, while the upper tropospheric humidity, as indicated by the NCEP reanalysis at 300 hPa, is roughly 10% greater than that over land (MINNIS ET AL. 2004). Thus, the atmosphere over pristine oceanic regions should be more susceptible to contrail-cirrus cloud initiation than that over land areas. Additionally, transoceanic flights travel greater lengths at high altitudes than their continental counterparts and, therefore, should tend to produce longer contrails. The expected average linear contrail coverage from theoretical considerations for 1992 air traffic (SAUSEN ET AL. 1998) varies between 0% in the mid-Pacific and 1% near San Francisco Bay (Fig. 1a). The nominal flight corridors are well defined by the theoretical contrail coverage in Figure 1a; those in the eastern half of the do-

[1] *Corresponding author:* Patrick Minnis, MS 420, NASA Langley Research Center, Hampton, VA, USA 23681. Email: p.minnis@nasa.gov

main are very similar to those seen in the more recent flight dataset of GARBER ET AL. (2004), which only includes flights east of 135°W. Cirrus coverage rose between 0 and 0.6%/year between 1971 and 1996 (MINNIS ET AL. 2004) over the same area, with a maximum increase over northern California (Fig. 1b). Over the ocean, a broad area with the greatest trends in cirrus coverage is centered near 45°N at the western edge of the domain in Figure 1. There is no obvious correlation between the cirrus trends and the theoretically derived contrail coverage. Understanding how the contrails relate to the changes in cirrus coverage necessitates the development of some empirical data on the linear contrail coverage. To begin that effort, this paper presents analyses of contrail properties as derived from satellite data over the North Pacific. The retrievals are compared to similar quantities derived from data over the continental United States of America (USA) and other areas to examine the differences between contrails formed over marine and continental areas. They are also compared to the theoretical results to determine the accuracy of models for predicting persistent contrails over the North Pacific.

2 Data and analysis

The 1-km window channel data from the Advanced Very High Resolution Radiometer (AVHRR) on the *NOAA-16* satellite are analyzed here using an automated detection method. Figure 2 shows examples of large contrails evident in the *NOAA-16* AVHRR imagery off the coast of California. Some of the trails exceed 1000 km in length and 20 km in width and they are evident in both the channel-4 infrared (IR, 11 μm) image (Fig. 2a) and, in Figure 2b, the 11-12 μm brightness temperature difference (T4-T5), a parameter that is used to differentiate contrails from cirrus clouds. The contrails in Figure 2 represent many different stages of growth and dissipation. Having lost much of their distinct linearity, many of the older contrails are difficult to distinguish from natural cirrus clouds.

The automated algorithm of MANNSTEIN ET AL. (1999) was applied to the afternoon *NOAA-16* data taken over the domain bounded by 25° - 55°N and 120° - 150°W (Fig. 1) during May, August, and November 2002 and February 2003. These 4 months should be representative of the four seasons and provide an estimate of the annual mean contrail properties. PALIKONDA ET AL. (2004) discuss the application of the detection method. In this study, the domain was divided into 12 regions that were used separately for a given application of the methodology. Contrail visible optical depth was computed for each pixel identified as a contrail with the method of MEYER ET AL. (2002) assuming that the contrail temperature is 224 K and that the contrail emissivity ε varies with optical depth (OD) for a given cosine of satellite viewing zenith angle, μ, according to the model of MINNIS ET AL. (1993) for small ice crystals:

$$\varepsilon = 1 - \exp[-0.458(OD / \mu)^{1.033}]. \qquad (1)$$

Contrail longwave radiative forcing (CLRF) and the background temperature were computed using the methods of PALIKONDA ET AL. (2002, 2004).

3 Results

Figure 3 shows the distribution of contrail coverage over the domain for the 4 months. The derived contrail coverage appears to distributed relatively homogeneously during February (Fig. 3a) except for extremes of both signs over the western third of the domain. During May (Fig. 3b), the heavy coverage appears to be confined mainly to the coastal routes (see Fig. 1a) with some lesser amounts along the southwestern and western corridors. During August (Fig. 3c), the greatest contrail coverage occurred around 47°N, 142°W with a secondary maximum near the west-southwest approach to San Francisco. More coverage occurs in northern part of domain in general. Minimum

coverage is seen in the southwestern corner of the domain, off the Oregon coast and inland. By November (Fig. 3d), the contrails occur primarily over the southern half of the domain and along the coastal routes. Overall, the observed mean contrail amounts were 0.67, 0.56, 0.51, and 0.51% during February, May, August and November, respectively.

The annual average distribution of contrail coverage (Fig. 4), based on the results in Figure 3, reveals that the persistent contrails were concentrated near the coast and west of northern California between 35°N and 42°N and along the coast and the northwestern corner of the domain. Contrails were rarely detected along the southwest-to-northeast diagonal of the domain and off the southern California coast. The annual mean coverage between May 2002 and February is 0.56%.

The frequency distributions of contrail *OD* and normalized CLRF (NCLRF) are plotted in Figure 5. *OD* (Fig. 5a) varies according to a slightly skewed Gaussian distribution with a mode value around 0.30. Smaller values ($OD < 0.20$) are more common during February and May while thicker contrails ($OD > 0.40$) are more frequent during the summer and fall. The minimum and maximum mean ODs, 0.22 and 0.28, occur during May and November, respectively, bounding the annual mean of 0.26. The NCLRF distribution (Fig. 5b) is highly skewed with a mode near 8 Wm^{-2}. The smallest values are more common during winter and spring than during the rest of year. Conversely, NCLRF > 15 Wm^{-2} occurs more often during August and November. NCLRF ranges from 13.5 Wm^{-2} in February to 17.4 Wm^{-2} during August with an annual average of 15.2 Wm^{-2}. The monthly mean CLRF only varies from 0.08 to 0.09 Wm^{-2} yielding an annual mean value of 0.085 Wm^{-2}. The large variability in NCLRF arises from the large range in background radiating temperatures. Contrails mixed with other cirrus clouds will tend to have small values of NCLRF while over clear areas NCLRF will be much larger, especially over land during the afternoon.

4. Discussion

The automated detection method is based on values of T4-T5 that produce a linear feature in the image. This assumption of linearity can cause both under- and overestimates of contrail coverage. Contrails do not always maintain linearity causing the technique to miss some contrails. Natural clouds, rivers, and coastlines can also produce linear features that can be mistaken as contrails. The technique is also sensitive to background variations and to minor peculiarities in the relative calibrations of the AVHRR channels 4 and 5. Thus, it is essential to estimate the errors in the detection method for each satellite and region analyzed.

To effect the detection error analysis, a user-interactive computer program was developed to display the T4 and T4-T5 images with removable red overlays of the automatically detected contrails. With the program, the analyst can evaluate the results both objectively by comparing T4 and T4-T5 values for the contrails with the surroundings and subjectively using contrast adjustment. Contrail pixels can be added or deleted based on the analyst's judgment. Deletions are made by selecting a rectangular box containing the false contrails and hitting the "delete" button. Additions are made for a selected box by setting T4 and T4-T5 thresholds to convert pixels having the encompassed values into contrail pixels. The thresholds can be adjusted until the resulting contrail pixels are satisfactory. Results are stored as images with the remaining, deleted, and added contrail pixels. The contrail properties can then be computed for all three categories.

Because the interactive analysis is labor intensive, only data for *NOAA-16* overpasses taken during 3 randomly selected days were analyzed for each month. Although this type of analysis is unavoidably subjective, the procedure follows some general guidelines. Among others, these include ensuring that the contrail is colder than the background and T4-T5 exceeds the background average, being aware of the air traffic corridors (contrails should not commonly occur with no air traffic), and assuming that contrails will generally not be oriented with the natural cirrus clouds (unless the air

traffic follows the orientation). Subjective analysis of the images is difficult especially when cirrus and contrails occur together. When it was not possible to decide if the pixels were actually contrails or cirrus, the automated result remained intact. The greatest overestimates generally occurred over the western portion of the domain as a result of cirrus streamers from cyclonic storms. Other common sources of overestimation are coastlines, rivers, cumulus streets, and cloud edges at high view angles. Underestimates generally occurred in contrail clusters, for older or faint contrails, and along the image edges because the method does not use the outer 10 pixels of the image. Pixels around the intersection of contrails were often missed. Although there was no attempt to explicitly add the cloudy pixels that were obviously from spreading contrails, some of those pixels were included in the additions because of variability in the required threshold for each contrail pixel. Conversely, some narrow contrails were not added for the same reason.

The results of the interactive analysis indicate that, relative to the number of detected contrail pixels, the method detected false contrails in 15 and 34% of the cases during May and February, respectively, with 22% for the other 2 months. On the other hand, 6-7% of the contrails were missed during November and February compared to 15 and 20% during May and August, respectively. Assuming that the results are representative of all of the analyzed images, it is possible to estimate correction factors to remove the biases. These factors, defined as the ratio of the number of deleted-to-original pixels multiplied by the ratio of the number of added-to-original contrail pixels, are 0.71, 1.00, 0.93, and 0.83, for February, May, August, and November, respectively. The resulting corrected monthly and annual mean contrail coverages are listed in Table 1 along with the original values. The corrected annual mean for the *NOAA-16* overpass time is 0.48%, a value 14% less than the raw, observed average.

Overall, contrail *OD* dropped somewhat when the false contrails were removed and the missed ones were added. The frequency distribution of the *OD*s for the error analysis dataset (Fig. 6a)

shows that the deleted pixels tend to have slightly larger *OD*s than the remaining pixels and the added pixels were generally thinner than the original ones. The relative frequency of added pixels in the lowest *OD* category is twice that for the remaining and deleted pixels while the frequency of larger *OD*s is reduced. Overall, the *OD*s for the adjusted contrails are 1 - 8% less than those for the original dataset. Correction factors were derived from the error analysis dataset and applied to the raw observations. The results given in Table 1 show that the *OD*s are still at a minimum in May and the corrected annual mean *OD* is 0.24. The corrected histogram of *OD*s plotted in Figure 6b shows the increase in thin cloud optical depths and decrease in thicker contrails relative to the annual mean. Figure 6b also confirms that the sampled error analysis dataset (denoted Original) is representative of the entire dataset. Table 1 includes the monthly and annual mean values of NCLRF. On average, NCLRF is reduced by 9% from 15.2 to 14.2 Wm^{-2}.

The original analysis did not include any pixels with $OD > 1$ as a means of eliminating some false positive detections. However, the error analysis, performed without the *OD* restriction, revealed that roughly 1 - 2% of the remaining and added pixels had $OD > 1$. Thus, the corrected means for all of the parameters in Table 1 are slightly underestimated by 1 - 2%. It should also be noted that the determination of the background radiances used to compute *OD* and *NCLRF* can include pixels containing cirrus produced as a result of spreading contrails. In such cases, both *OD* and *NCLRF* will be underestimated.

An additional coverage correction is necessary because the afternoon *NOAA-16* sampling is not representative of the daily average air traffic over the Pacific. From the database of GARBER ET AL. (2004), it was determined that for the 3 hours straddling 2030 UTC, roughly 1 hour before *NOAA-16* passes over the center of the domain, the number of flights and cumulative flight length are 30% greater than the corresponding 24-hour means. Assuming that contrail formation conditions are independent of the time of day over a 1 month period, then the mean observed contrail coverage

should be multiplied by 0.7. Thus, the best estimate of mean contrail coverage for the domain is 0.34 as shown in Table 1. Additional data from satellites with other overpass times should be analyzed to test the assumption of uniform conditions over the day.

The diurnally corrected mean annual contrail coverage for the domain is comparable to its theoretical counterpart of 0.30 (SAUSEN ET AL. 1998). If it is assumed that air traffic over the domain has increased by 2.5% per annum since 1992, the air-traffic year used by SAUSEN ET AL. (1998), and the contrail coverage increased by the same amount, then the theoretical coverage would be ~ 0.37. Thus, the best estimate from the *NOAA-16* analysis agrees to within ±10% with the theoretical contrail coverage. The theoretical calculations of PONATER ET AL. (2002) suggest that summertime contrail coverage over the area should be slightly larger than that during winter. The current results agree in that the May and August means are 14% greater than the average for the other 2 months. From the error analysis, it was found that most of the false detections occurred over the western portion of the grid where air traffic is minimal. Removal of those false contrails from Figure 4 would result in better agreement between the theoretical and observed contrail coverage distributions.

The contrail optical depth distributions and mean values are nearly identical to those derived over the USA by PALIKONDA ET AL. (2004). The means are more than twice the magnitude found over Europe by MEYER ET AL. (2002) and estimated by PONATER ET AL. (2002) from theoretical calculations. Although the differences may be related to mistaken cirrus clouds that are deeper than the average contrail, it is clear from the error analysis that the current *OD* values are fairly robust. The smaller values over Europe may be due to a less-than-average value of supersaturation available for contrail growth while the theoretical calculations may underestimate *OD* in parts of the globe.

The February NCLRF mean is 5 Wm^{-2} greater than the wintertime mean for *NOAA-16* results over the USA while the August NCLRF is 2 Wm^{-2} less than the corresponding USA summertime mean (PALIKONDA ET AL. 2004). This seasonal difference in NCLRF is likely due to the relatively sta-

ble background temperatures over the ocean. Over land, the contrast between the contrail and surface temperatures is much greater in summer than in winter. The mean value of NCLRF is nearly identical to the net radiative forcing computed for the zone between 25°N and 55°N from the data of MINNIS ET AL. (1999) using *OD* = 0.25. Based on the ratio of the longwave to net forcing, the NCLRF from that study would be ~22 Wm^{-2} or 50% greater than the value seen here. It is not clear that the Northeast Pacific domain is representative of the entire latitudinal band. If it is, then it is likely that the observed contrails occur more frequently over high clouds than assumed by MINNIS ET AL. [1999].

3 Concluding remarks

The results presented here constitute the first objective analysis of linear contrails over the eastern North Pacific. After correction for errors, the contrail coverage is in excellent agreement with the amount derived theoretically. However, the corrected optical depths are twice as large as those derived over Europe from satellite data and from theoretical calculations. Contrail longwave radiative forcing appears to be much greater than computed theoretically. Further study is required to understand the various discrepancies. Nevertheless, the results provide another point of validation for the global estimation of contrail coverage.

Future studies of contrails over this area should also compute the shortwave radiative forcing to obtain the net forcing by contrails. Shortwave forcing is more complex to estimate because of the greater impact of the diurnal cycle on the relative albedos of the contrail and the underlying background. To better understand diurnal and interannual variability in contrail properties, additional analyses should be performed including data from other NOAA satellites and the NASA *Terra* and *Aqua* satellites to improve diurnal coverage. Error analyses that pinpoint the locations of false detections should also be undertaken to facilitate further comparisons of model and satellite-derived parameters. The new tool developed for interactive contrail analysis may also prove valuable for

measuring the extent of contrail spreading, thus providing a more comprehensive assessment of the impact of contrails on climate. The results of this study will be compared with the model-predicted temperature and humidity conditions to help improve the parameterization of contrails in climate models so that a more accurate assessment of contrail effects can be computed for the northeastern Pacific Ocean.

Acknowledgments

This research was supported by the NASA Pathfinder Program and the NASA Office of Earth Science Radiation Sciences Program. The original air traffic summary was provided by Don Garber.

References

GARBER, D. P., P. MINNIS, and P. K. COSTULIS, 2004: A USA commercial flight track database for upper tropospheric aircraft emission studies. - Meteorol. Z., submitted.

MANNSTEIN, H., R. MEYER, and P. WENDLING, 1999: Operational detection of contrails from NOAA AVHRR data. - Int. J. Remote Sens., **20**, 1641-1660.

MEYER, R., H. MANNSTEIN, R. MEERKÖTTER, U. SCHUMANN, and P. WENDLING, 2002: Regional radiative forcing by line-shaped contrails derived from satellite data. - J. Geophys. Res., **107**, D10 10.1029/2001JD000426.

MINNIS, P., J.K. AYERS, R. PALIKONDA, and D. PHAN, 2004: Contrails, cirrus trends, and climate. - J. Climate, in press.

MINNIS, P., U. SCHUMANN, D. R. DOELLING, K. M. GIERENS, and D. FAHEY, 1999: Global distribution of contrail raditive forcing. - Geophys. Res. Lett., **26**, 1853-1856.

MINNIS, P., Y. TAKANO, and K.-N. LIOU, 1993.: Inference of cirrus cloud properties using satellite-observed visible and infrared radiances, Part I: Parameterization of radiance fields. - J. Atmos. Sci., **50**, 1279-1304.

PALIKONDA, R., P. MINNIS, P. K. COSTULIS, and D. P. DUDA, 2002: Contrail climatology over the USA from MODIS and AVHRR data. *Proc. 10th Conf. on Aviation, Range, and Aerospace Meteorology*, Portland, OR, May 13-16, J9-J12.

PALIKONDA, R., P. MINNIS, D. P. DUDA, and D. N. PHAN, 2004: Contrail coverage over the USA from AVHRR data. - Meteorol. Z., submitted.

PONATER, M., S. MARQUART, and R. SAUSEN, 2002: Contrails in a comprehensive global climate model: parameterisation and radiative forcing results. - J. Geophys. Res., **107**, 10.1029/2001JD000429.

SAUSEN, R., K. GIERENS, M. PONATER, M. and U. SCHUMANN, 1998: A diagnostic study of the global coverage by contrails, part I, present day climate. - Theor. Appl. Climatol. **61**, 127-141.

Table 1. Summary of contrail properties for North Pacific domain, May 2002 - February 2003.

	Contrail Coverage (%)			Optical Depth		NCLRF (Wm^{-2})	
	raw	corrected	diurnal	observed	corrected	observed	corrected
February	0.67	0.48	0.34	0.27	0.25	13.5	12.8
May	0.56	0.56	0.39	0.22	0.20	13.9	13.1
August	0.51	0.47	0.33	0.26	0.26	17.4	16.1
November	0.51	0.42	0.30	0.28	0.26	16.1	14.8
Annual	0.56	0.48	0.34	0.26	0.24	15.2	14.2

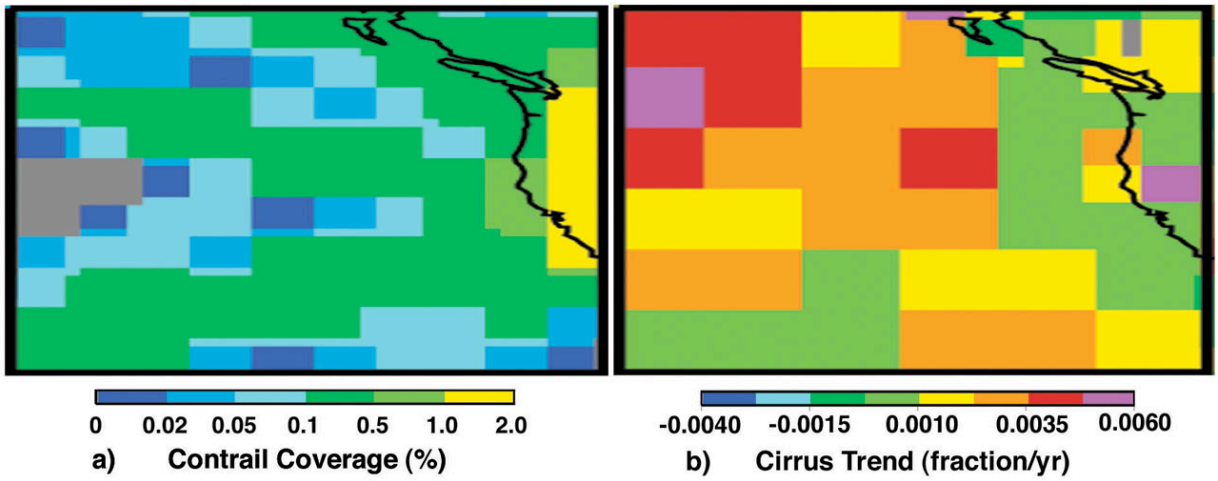

Fig. 1. Theoretical linear contrail coverage in 1992 (a) and trend in surface-observed 1971-1996 cirrus coverage (b).

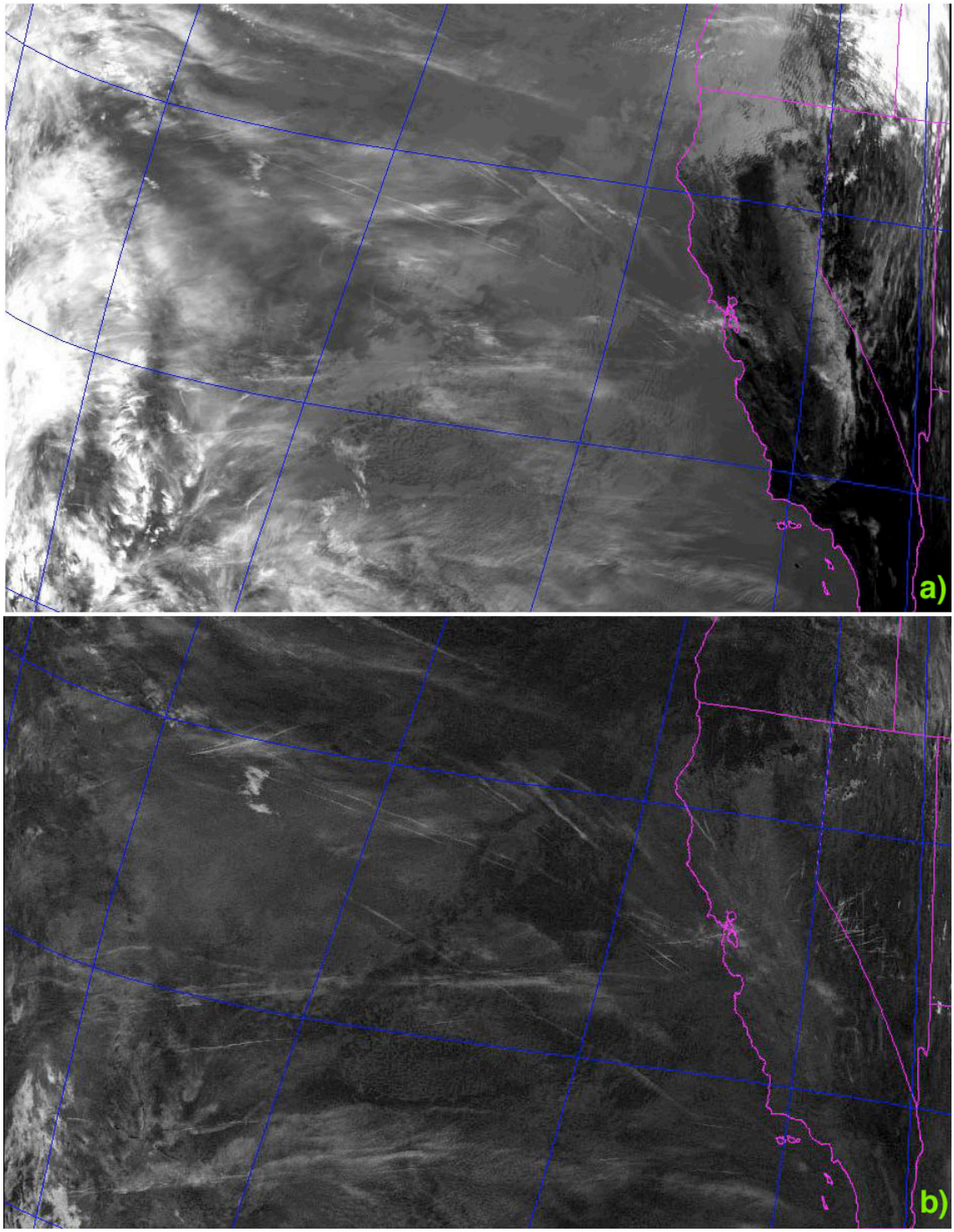

Fig. 2. *NOAA-16* AVHRR imagery at 2100 UTC, 21 February 2003: (a) Infrared brightness temperature and (b) channel 4-5 brightness temperature difference.

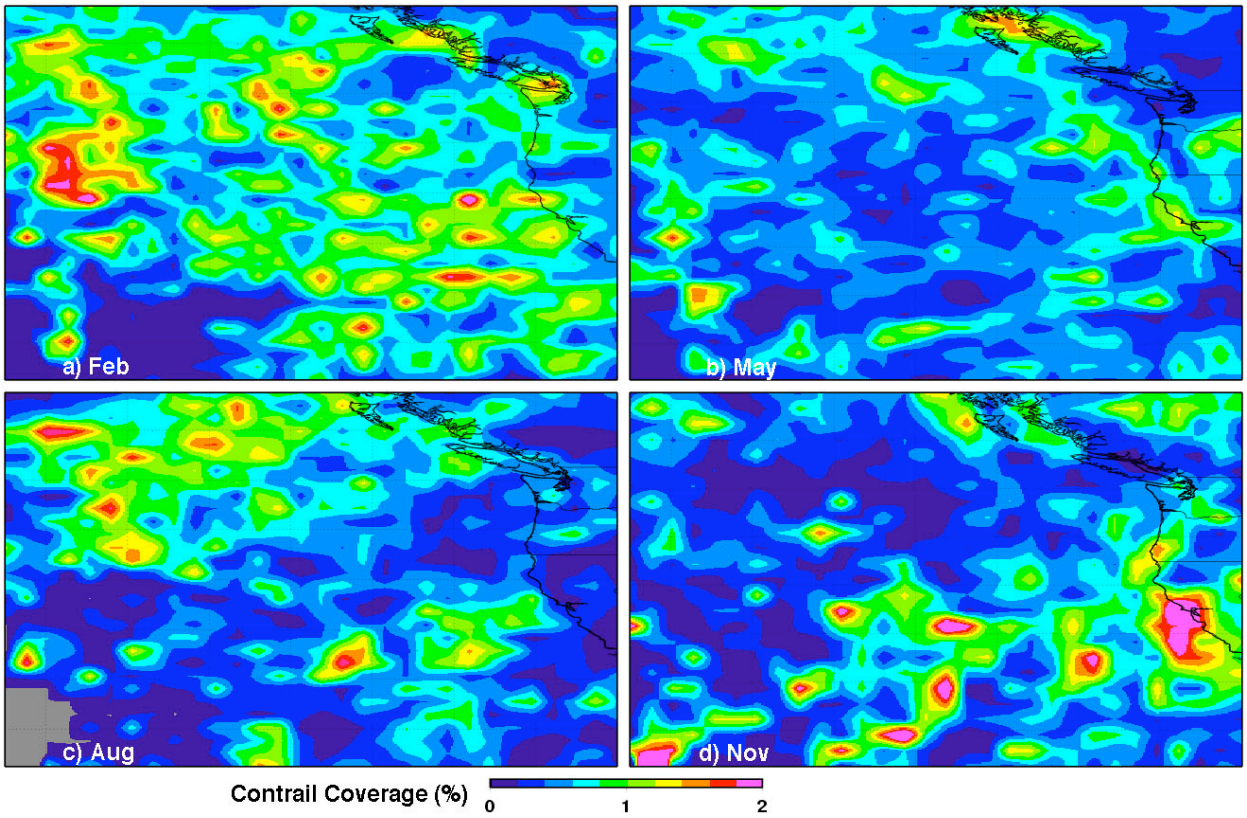

Figure 3: Monthly mean contrail coverage derived from afternoon (1430 LT) NOAA-16 AVHRR data during 2002 (b-d) and 2003 (a).

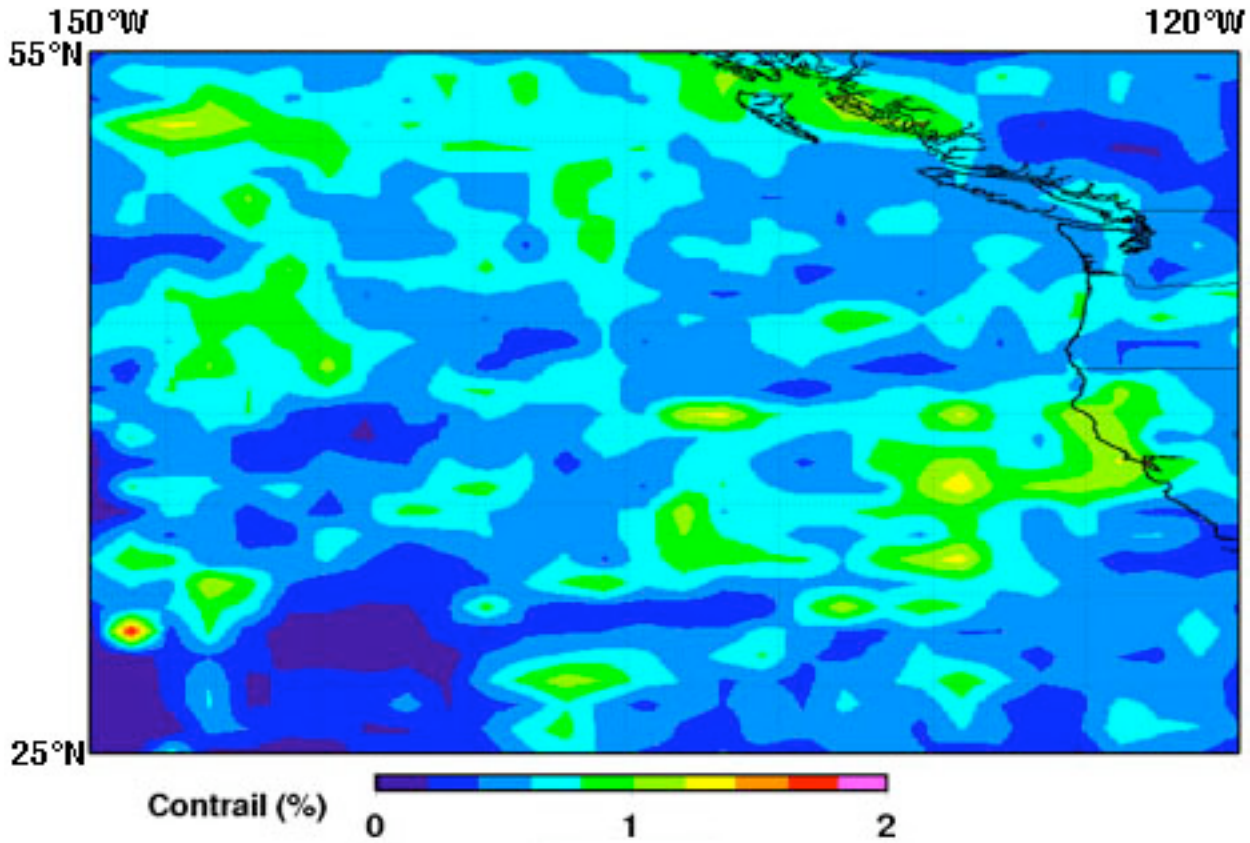

Figure 3: Monthly mean contrail coverage derived from afternoon (1430 LT) NOAA-16 AVHRR data during 2002 (b-d) and 2003 (a).

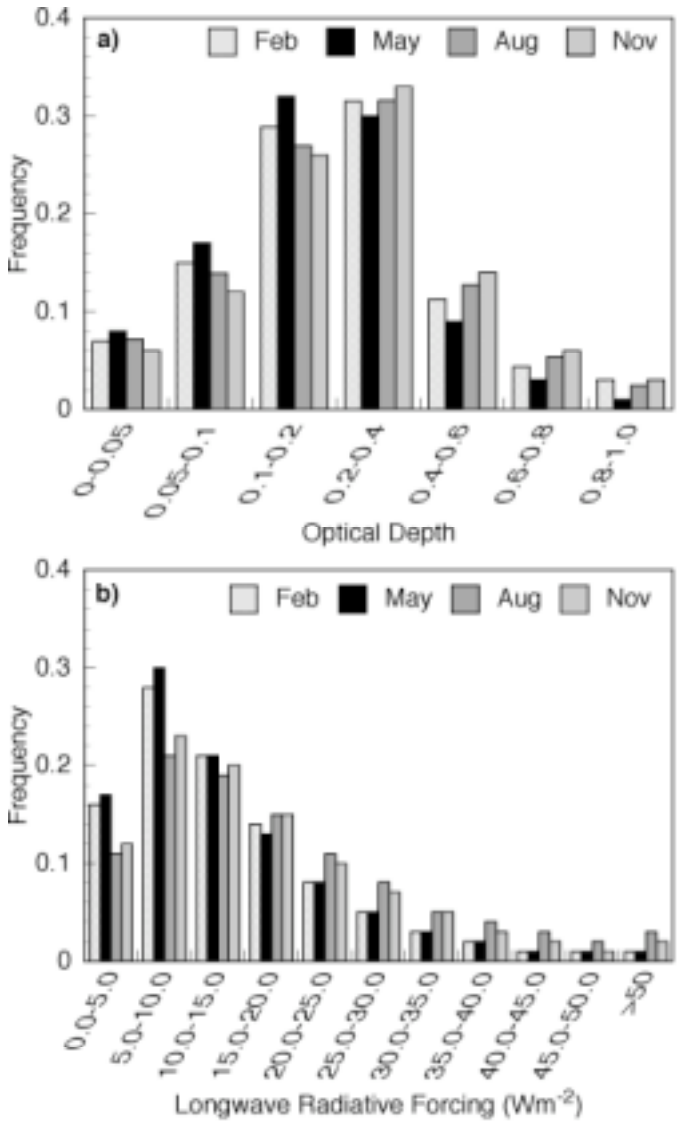

Figure 5. Frequency distributions of (a) contrail optical depth and (b) NCLRF during February 2003.

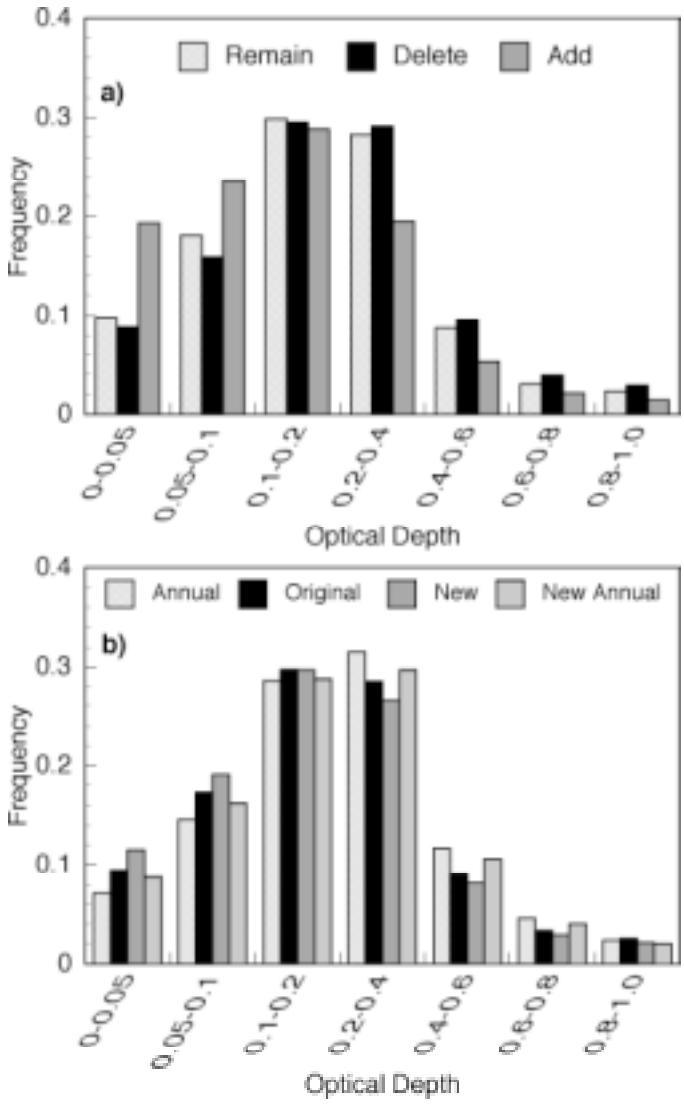

Fig. 6. Frequency distributions of contrail optical depths for (a) error analysis dataset and (b) domain annual mean (annual) and corrected annual mean (new annual) and error analysis original dataset (remaining plus deleted = original) and corrected (remaining plus added = new).